bioRxiv preprint doi: https://doi.org/10.1101/464784; this version posted November 20, 2018. The copyright holder for this preprint (which was not certified by peer review) is the author/funder. All rights reserved. No reuse allowed without permission.

NEUROIMAGING SUPPORTS THE REPRESENTATIONAL NATURE OF THE EARLIEST HUMAN ENGRAVINGS

Mellet E[1,2,3]* · Salagnon M[1,2,3] · Majki A[4] · Cremona S[1,2,3] · Joliot M[1,2,3] · Jobard G[1,2,3] · Mazoyer B[1,2,3] · Tzourio Mazoyer N[1,2,3] · d'Errico F[4,5]

Submitted on 7 November 2018

Abstract The earliest human graphic productions dating to the Lower and Middle Palaeolithic are associated with anatomically modern and archaic hominins. These productions, which consist of abstract patterns engraved on a variety of media, may have been used as symbols, and their emergence is thought to be associated with the evolution of the properties of the visual cortex. To test this hypothesis, we used functional magnetic resonance imaging to compare brain activations triggered by the perception of engraved patterns dating between 540,000 and 30,000 years before the present with those elicited by the perception of scenes, objects, symbol-like characters, and written words. The perception of the engravings bilaterally activated regions in the ventral route in a pattern similar to that produced by the perception of objects, suggesting that these graphic productions are processed as organized visual representations in the brain. Moreover, the perception of the engravings led to a leftward activation of the visual word form area. These results support the hypothesis that in contrast to random doodles, the earliest abstract graphic productions had a representational purpose for modern and archaic hominins.

Keywords Human evolution · Symbols · Engravings · Perception · Ventral pathway · fMRI

Corresponding author:

Emmanuel Mellet

emmanuel.mellet@u-bordeaux.fr

[1] Univ. Bordeaux, IMN, UMR 5293, F-33000 Bordeaux, France

[2] CNRS, IMN, UMR 5293, F-33000 Bordeaux, France

[3] CEA, GIN, IMN, UMR 5293, F-33000 Bordeaux, France

[4] PACEA UMR 5199, Univ. Bordeaux, CNRS, Pessac, France

[5] SFF Centre for Early Sapiens Behaviour (SapienCE), University of Bergen, Bergen, Norway

From Palaeolithic rock paintings to contemporary art, abstract and figurative graphic productions have represented a major aspect of human cognitive activity. The ability to produce visual representations was assumed to have emerged at the beginning of the Upper Palaeolithic era approximately 42,000 years BP (Before Present) due to a sudden genetic mutation occurring only in anatomically modern human populations1. The subsequent discoveries of abstract paintings and engravings older than 42,000 years in Africa and Eurasia suggest that this ability emerged much earlier and was shared by different fossil species, including *Homo erectus*[2], Neanderthals[3,4] and Early *African Homo sapiens*. Analyses of several early abstract patterns have shown that these patterns were produced deliberately and had no apparent utilitarian function[2,3,5,6], leading some authors[7] to argue that these ancient abstract patterns represent the earliest instances of symbol use a thousand years prior to the earliest known 40- to 30,000-year-old examples of depictional representations[8]. The production of abstract patterns has been linked to the evolution of the primary visual areas and surrounding cortex[9,10]. Alternatively, the complexification of graphic productions from simple geometric to depictional representations may reflect the successive evolutionary stages of visual information processing through the primary visual cortex to the occipito-temporal cortex via the ventral route. The ventral route is involved in the extraction of visual information and allows the recognition of visual categories, such as shapes, scenes, and words (see[11] and[12] for a review). If the abstract patterns intentionally engraved by hominins were not random doodles and were perceived as structured forms with a potential meaning, their perception should engage the ventral route cortex, which extends anteriorly to the early visual areas in the occipito-temporal pathway. We test this hypothesis in the present study, which aims to characterize the cerebral regions involved in the perception of the earliest engraved abstract graphisms (EEAG). The blood oxygen level dependent (BOLD) signal was mapped in

bioRxiv preprint doi: https://doi.org/10.1101/464784; this version posted November 20, 2018. The copyright holder for this preprint (which was not certified by peer review) is the author/funder. All rights reserved. No reuse allowed without permission.

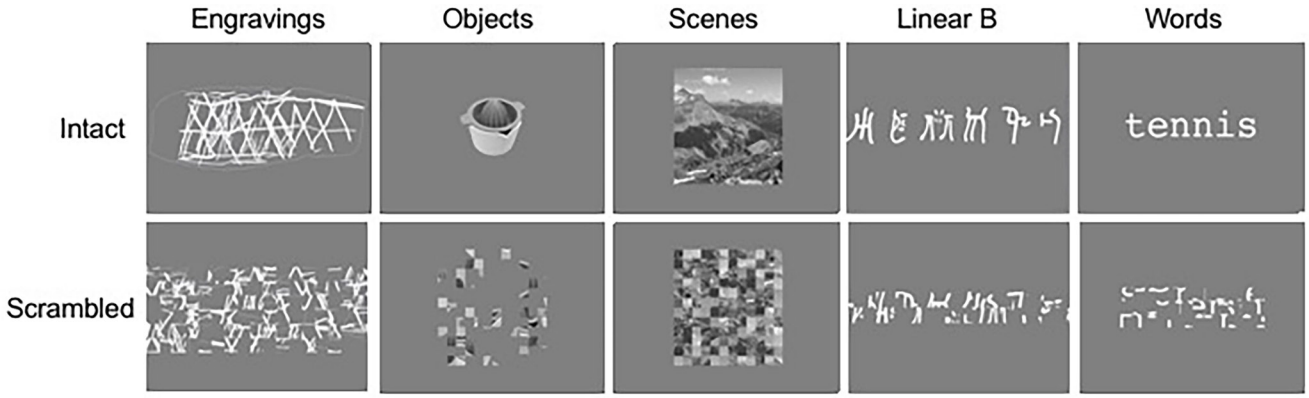

Figure 1. Example of intact and scrambled stimuli used in the 1-back task.

twenty-seven healthy volunteers using functional magnetic resonance imaging (fMRI), while the individuals were presented with tracings of EEAG dating between 540 ka and 30 ka (See Table S1). The perception of these patterns was compared to the perception of their scrambled version, in which the genuine organization of the abstract patterns was lost to assess whether the geometric organization of the EEAG (albeit some patterns were very simple) could be differentiated at the visual cortex level from patterns with no perceptual organization. Another aim of the study was to shed light on the nature of the EEAG. Therefore, we assessed whether the regions activated by the perception of EEAG were also involved in the processing of other visual categories visually presented to the same participants, including a scrambled version of each stimulus belonging to each categoriy (Figure 1).

The first category included pictures of nameable human-made artefacts. These stimuli conveyed semantic and lexical information but no symbolic content. The rationale for this choice is that proximity between the patterns of activation of the EEAG and objects could support the representational character of the EEAG, which could also indicate that the EEAG were processed as a whole rather than a collection of lines, fulfilling the "good shape" criteria of the gestalt theory of perception[13,14]. The second category was represented by outdoor scenes depicting large-scale surroundings. These stimuli provided information regarding the outer world and conveyed semantic content without being perceived as a single item. In addition, two symbolic categories were included in the study. The first symbolic category included chains of characters from the linear B syllabic script, which is a writing system unknown to the participants, and these characters were chosen as stimuli perceptible as 'potentially' symbolic. A similar profile of activation between the EEAG and linear B script stimuli could suggest that the EEAG are processed as symbols or signs that result from a combination of structurally simple elements. The second symbolic category was represented by two-syllable words. This condition extended the requirements of processing the linear B alphabet because the perception of familiar individual overlearned signs (letters) and familiar combinations trigger access to the pronunciation and meaning of words. In addition, word reading is characterized by a leftward asymmetric activation of the ventral route that reflects symbol processing and lexical and semantic access[15,16]. Thus, this condition provides a pattern of leftward asymmetry that could be compared with the asymmetry elicited by the perception of EEAG. The regional BOLD values in response to the engravings *minus* the scramble contrast were extracted from each homotopic region (hROI) of the functional homotopic atlas AICHA[17]. The regions included in the analysis fulfilled the following two criteria: in at least one hemisphere, a significant positive value was observed in response to both the engravings minus scramble contrast ($p < 0.05$ False discovery rate, FDR corrected, one-sample two-sided t-test) and engravings minus fixation (see methods) contrast ($p < 0.05$ uncorrected, one- sample two-sided t-test). The fulfilment of these conditions ensured that regions with stronger deactivation under the reference condition (Scramble) during the EEAG comparison with the fixation were not selected.

Ten hROIs were significantly activated in either the right or left hemisphere in the engravings minus scramble contrast. All hROIs were located in the visual ventral pathway (Table 1, Table S2 and Figure 2). Thus, the perceptual processing of EEAG compared to their scrambled version did not involve primary visual areas but did involve visual regions beyond the primary visual and peristriate areas. Previous work has led authors to propose that the early visual cortex may play a role in the extraction of the geometric features composing EEAG[9,10]. However, the present work shows that the activity

bioRxiv preprint doi: https://doi.org/10.1101/464784; this version posted November 20, 2018. The copyright holder for this preprint (which was not certified by peer review) is the author/funder. All rights reserved. No reuse allowed without permission.

	OLat3	O2-2	O3-2	O3-1	T3-5	FUS5	T3-4	FUS4	FUS3	FUS2
					Engravings					
BOLD LH	0.25 (0.11)*	0.16 (0.06)*	0.46 (0.09)*	0.49 (0.09)*	0.27 (0.07)*	0.20 (0.05)*	0.31 (0.08)*	0.39 (0.08)*	0.18 (0.04)*	0.13 (0.05)*
BOLD RH	0.45 (0.16)*	0.17 (0.07)*	0.43 (0.10)*	0.36 (0.10)*	0.16 (0.06)*	0.25 (0.07)*	0.19 (0.11)*	0.28 (0.09)*	0.13 (0.04)*	0.12 (0.04)*
Asym L-R	-0.20 (0.09)	0.00 (0.03)	0.03 (0.06)	0.13 (0.06)	0.11 (0.04)	-0.05 (0.04)	0.13 (0.06)	0.12 (0.04)*	0.05 (0.02)	0.00 (0.03)
					Objects					
BOLD LH	0.37 (0.08)*	0.11 (0.05)*	0.52 (0.07)*	0.55 (0.08)*	0.26 (0.05)*	0.34 (0.04)*	0.37 (0.07)*	0.43 (0.07)*	0.19 (0.04)*	0.19 (0.03)*
BOLD RH	0.48 (0.10)*	0.15 (0.05)*	0.41 (0.06)*	0.16 (0.07)*	0.12 (0.05)*	0.25 (0.04)*	-0.06 (0.07)	0.25 (0.05)*	0.10 (0.03)*	0.17 (0.03)*
Asym L-R	-0.11 (0.08)	-0.04 (0.03)	0.11 (0.05)*	0.40 (0.07)*	0.13 (0.04)*	0.08 (0.03)*	0.43 (0.04)*	0.19 (0.05)*	0.09 (0.02)*	0.02 (0.03)
					Words					
BOLD LH	-0.22 (0.06)*	-0.41 (0.05)*	-0.28 (0.06)*	-0.47 (0.08)*	-0.22 (0.05)*	-0.18 (0.03)*	-0.08 (0.07)	0.25 (0.06)*	0.07 (0.04)	0.07 (0.03)*
BOLD RH	-0.43 (0.08)*	-0.36 (0.06)*	-0.45 (0.07)*	-0.66 (0.06)*	-0.23 (0.04)*	-0.27 (0.04)*	-0.58 (0.08)*	-0.16 (0.05)*	-0.07 (0.03)*	0.04 (0.03)
Asym L-R	0.21 (0.06)*	-0.04 (0.04)	0.17 (0.04)*	0.19 (0.08)*	0.01 (0.06)	0.10 (0.04)*	0.50 (0.08)*	0.41 (0.04)*	0.14 (0.03)*	0.11 (0.03)*
					Linear B					
BOLD LH	0.32 (0.08)*	-0.02 (0.05)	0.33 (0.07)*	0.19 (0.09)*	0.06 (0.06)	0.14 (0.04)*	0.14 (0.07)	0.40 (0.07)*	0.14 (0.04)*	0.14 (0.04)*
BOLD RH	0.42 (0.10)*	0.01 (0.04)	0.26 (0.06)*	-0.01 (0.08)	0.01 (0.06)	0.04 (0.04)	-0.12 (0.07)	0.23 (0.04)*	0.11 (0.03)*	0.10 (0.03)*
Asym L-R	-0.10 (0.09)	-0.03 (0.04)	0.06 (0.04)	0.20 (0.06)*	0.05 (0.05)	0.10 (0.04)*	0.25 (0.05)*	0.17 (0.06)*	0.03 (0.02)	0.04 (0.03)
					Scenes					
BOLD LH	-0.02 (0.06)	0.21 (0.04)*	0.12 (0.04)*	0.07 (0.05)	0.06 (0.03)	0.31 (0.04)*	0.07 (0.05)	0.10 (0.05)	0.06 (0.03)	0.07 (0.02)*
BOLD RH	0.14 (0.06)*	0.20 (0.04)*	0.15 (0.05)*	0.00 (0.05)	0.09 (0.03)*	0.44 (0.05)*	-0.07 (0.06)	0.11 (0.04)*	0.10 (0.03)*	0.12 (0.02)*
Asym L-R	-0.16 (0.03)*	0.01 (0.03)	-0.04 (0.02)	0.07 (0.03)*	-0.04 (0.02)	-0.13 (0.04)*	0.14 (0.03)*	-0.01 (0.03)	-0.04 (0.02)	-0.05 (0.02)*

Table 1 Mean BOLD value of the ten hROIs activated in the engraving minus scramble contrast and left minus right asymmetry under the five conditions. * significant (one-sample test, $p < 0.05$ corrected).

generated by the perception of scrambled and intact EEAG in the early visual cortex does not substantially differ. This similarity suggests that the evolution of the properties of the primary visual cortex was unlikely to play a central role in the emergence of EEAG or that the latter triggered the former.

Although EEAG are not recognized as existing entities, their perception elicited activation in anterior regions of the ventral pathway sensitive to distinct visual categories[11,12,18,19]. Since the EEAG and their scrambled version differed because the latter lacked geometric organization, the level of perceptual organization required for EEAG appears to be sufficiently high to recruit higher order visual areas. The involvement of the visual ventral pathway indicates that information processing requires more than the mere identification of visual primitives, such as the simple extraction of edges, oriented segments, or ends of lines.

Interestingly, in the left hemisphere, the 10 regions activated in the EEAG *minus* scramble contrast were also significantly activated by the perception of objects compared to their scrambled version (Table 1 and Figure 2). Repeated-measures ANOVA comparing EEAG and object perception conditions showed that there was no hROIs x condition interaction effect on the BOLD values ($F(9,225) = 1.6$, $p = 0.11$), reflecting the similarity of activation between these two conditions in the left hemisphere. In the right hemisphere, a condition by region interaction was present ($F(9,225) = 2.4$, $p = 0.02$) due to a significantly lower BOLD value in the right inferior temporal hROI (T3-4) under the object condition than under the EEAG condition. No other regions showed a significant BOLD difference between these two conditions in the right hemisphere. The activation profile in response to each visual category compared to its scrambled version among the 10 hROIs confirms that the EEAG and object conditions triggered similar activations along the ventral pathway (Figure 3). Notably, the activation profile under the EEAG perception condition in the 16 hROIs activated by object perception (listed in Table S3 as supplementary material) was also identical (see figure S1 in supplementary material), providing supplementary evidence of the brain functional overlap between object and EEAG perception.

In contrast, the comparison of the BOLD values observed under the EEAG condition with those in each of the other conditions revealed strongly significant hROIs x conditions interactions in all cases in both the left [EEAG, LinearB: $F(9,225) = 3.6$, $p = 0.0003$), EEAG, Words: $F(9,225) = 23.6$, $p < 0.0001$, EEAG, Scenes ($F(9,225) = 13.9$, $p < 0.0001$)] and the right [EEAG, LinearB ($F(9,225) = 3.4$, $p = 0.0006$, EEAG, Words $F(9,225) = 18.0$, $p < 0.0001$, EEAG, Scenes ($F(9,225) = 11.4$, $p < 0.0001$)] hemispheres. Thus, the activation profile under the linear B script, words and scenes conditions compared to their scrambled version differed from that under the EEAG condition, although some regions exhibited the same level of activation (Figure 3A). The plot of activations under the EEAG condition against the activations under each of the other conditions suggests

bioRxiv preprint doi: https://doi.org/10.1101/464784; this version posted November 20, 2018. The copyright holder for this preprint (which was not certified by peer review) is the author/funder. All rights reserved. No reuse allowed without permission.

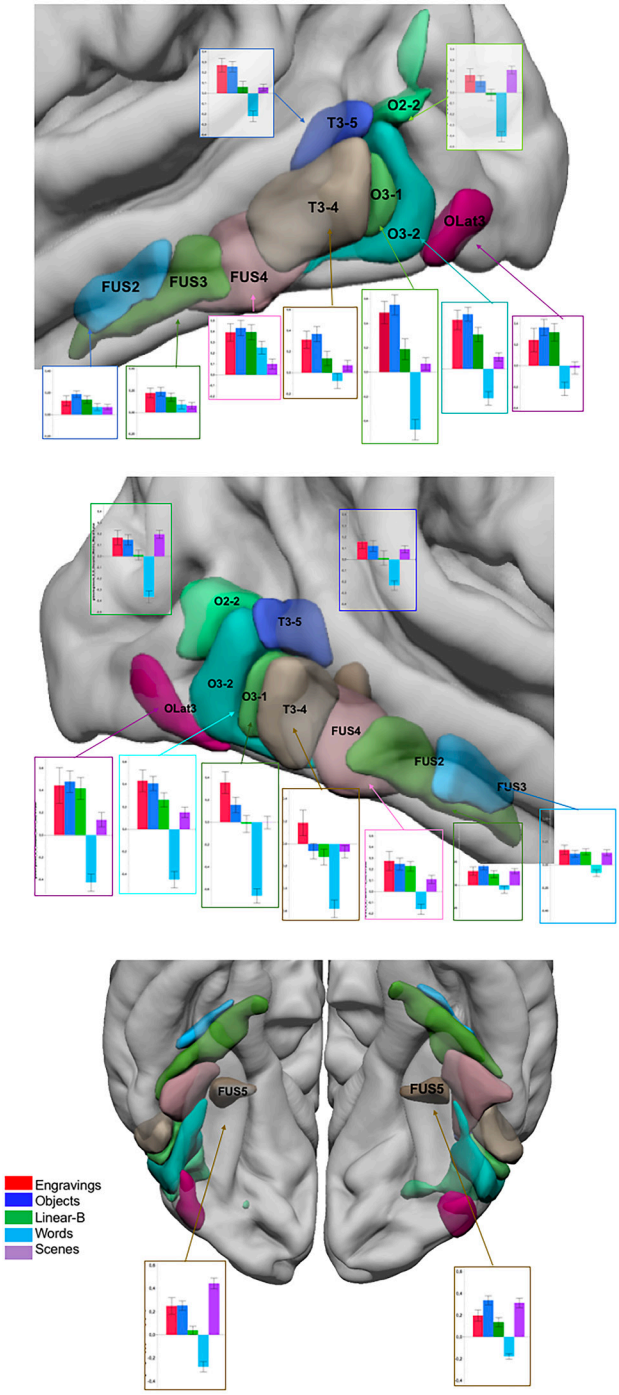

Figure 2. Superimposition on an MRI template of the 10 hROIs showing a significant BOLD signal increase in the engravings *minus* scramble contrast. **Top:** Lateral view of the left hemisphere, **Middle:** Lateral view of the right hemisphere, **Bottom:** Inferior view of the left and right hemispheres. Bar plots represent the BOLD values obtained in the five categories *minus* their scrambled version contrasts in each region. Error bars represent the standard error of the mean.

that a positive linear relationship exists only between the objects and EEAG conditions (Figure 3B).

To verify that the relationship observed at the group level between the activation profiles elicited by the objects and EEAG was not determined by outliers, the correlation of the activation profiles in 10 regions in response to the EEAG and objects (compared to their scrambled version) was computed in each hemisphere separately for each subject. Then, the resulting Pearson's correlation coefficients of each subject were Fisher z-transformed and analysed using a univariate two-sided t-test that was significant in both the left ($t(25) = 7.6$, $p < 0.0001$) and right ($t(25) = 4.8$, $p < 0.0001$) hemispheres. This finding confirms that both EEAG and object perception recruit the ventral pathway in a similar way in both hemispheres.

The proximity of the ventral visual cortex responses to these two visual categories was likely elicited by the global visual organization of EEAG, which triggered processes comparable to those required for object recognition. Among the regions activated by the perception of both EEAG and objects, O3-1 and O3-2 corresponded to the so-called LO functional region[20]. LO is defined as the brain area showing the greatest activation while viewing a known or novel object compared to its scrambled version[20,21]. The involvement of this region further supports the hypothesis that the processes involved in object recognition are involved in the perception of EEAG. This hypothesis is consistent with the fact that LO has been proven to be sensitive to the shape, but not the semantics, of objects[22,23]. Thus, although the similarity between the profiles of the objects and EEAG does not demonstrate that EEAG were previously used as symbols, modern brains perceive these EEAG as coherent visual entities to which symbolic meaning can be attached. Given that it has recently been argued that the anatomy of cortical areas belonging to the visual ventral cortex have been moderately impacted by the evolution of the brain from the earliest hominins to *Homo sapiens*[24,25], it seems reasonable to speculate that the present results also apply to early modern humans and archaic hominins. Considering that EEAG were produced deliberately and had no apparent utilitarian function, our results are consistent with the hypothesis that these graphic productions had a representational purpose and were used and perceived as icons or symbols by modern and archaic hominins.

At the regional level, only one area, i.e., the occipito-temporal region of the left hemisphere or FUS4, was activated by both EEAG and tasks involving symbolic or iconic contents (objects, linear B, and words). This region corresponds to the so-called visual word form area (VWFA)[26,15]. This region was activated by the perception of both objects, i.e., the linear B script and words, which is consistent with the proposal that the role of the left FUS4 is not restricted to word recognition[27–29]. As proposed by Vogel, FUS4 processing extends to the processing of complex visual perception with a statistical regularity

bioRxiv preprint doi: https://doi.org/10.1101/464784; this version posted November 20, 2018. The copyright holder for this preprint (which was not certified by peer review) is the author/funder. All rights reserved. No reuse allowed without permission.

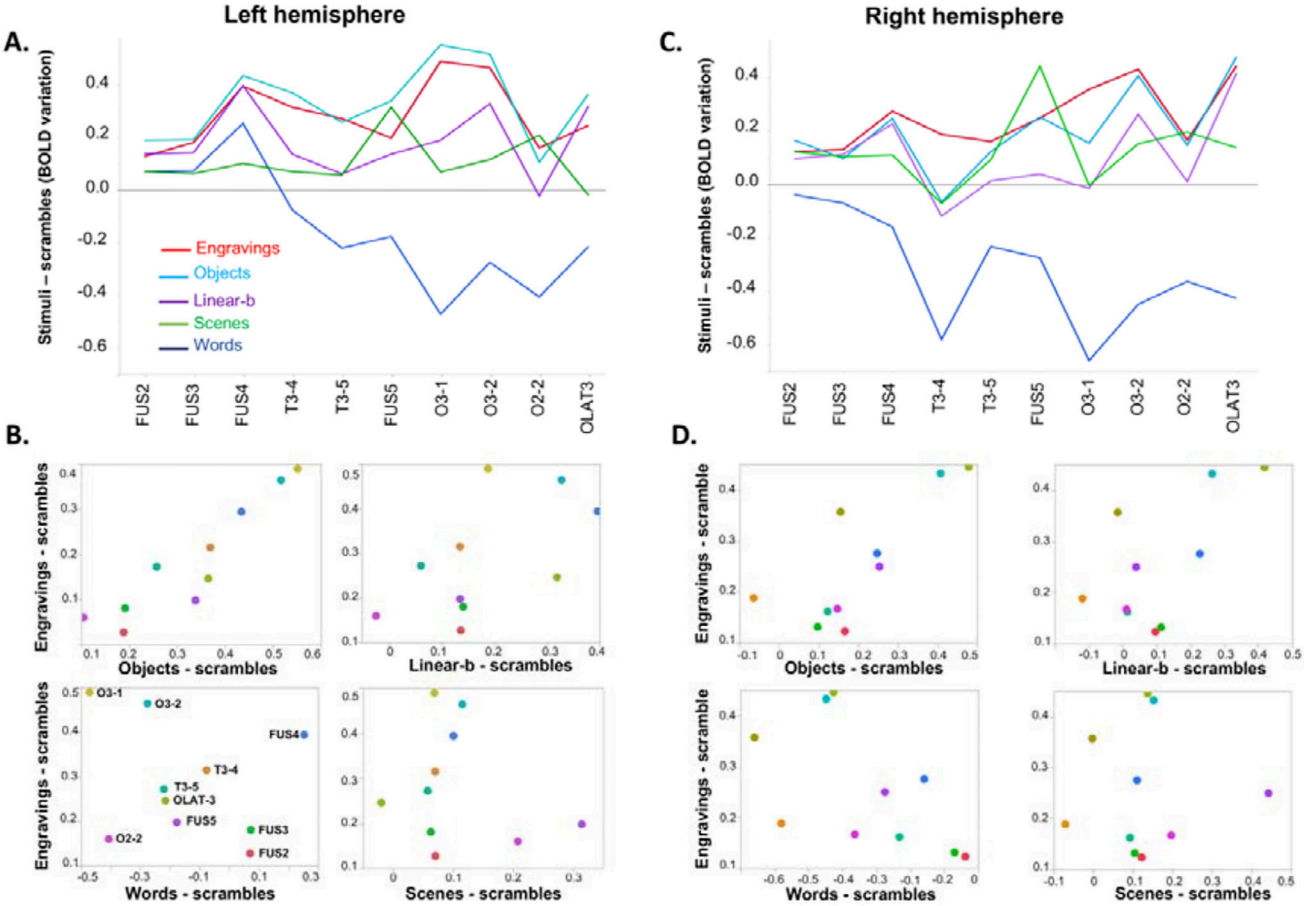

Figure 3. Descriptive analysis of the activation profiles of the 10 hROIs of the ventral route activated by EEAG perception under the different conditions. **Top:** Profiles of activity in the left hemisphere (**A**) and right hemisphere (**C**) in regions presented in an antero-posterior sequence along the ventral route. **Bottom:** Plots of the BOLD values obtained under the EEAG condition against those obtained under the objects, linear B words and scenes conditions across the 10 hROIs in the left (**B**) and right (**D**) hemispheres. Notably, the values on the horizontal axis can be positive, null, or negative according to the contrast and the hROIs.

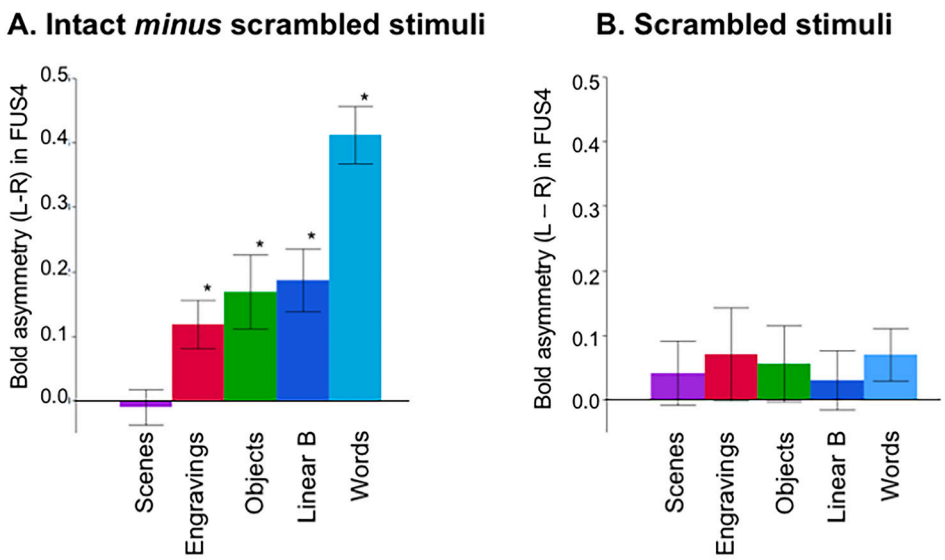

Figure 4. Asymmetries of BOLD signal (left minus right) in FUS4 under the five conditions **A.** Asymmetries measured in the contrast of intact minus scrambled stimuli. **B.** Asymmetries measured during the perception of the scrambled version of each category of stimuli (*: $p < 0.05$, one-sample t-test, FDR corrected. Error bars represent the standard error of the mean).

bioRxiv preprint doi: https://doi.org/10.1101/464784; this version posted November 20, 2018. The copyright holder for this preprint (which was not certified by peer review) is the author/funder. All rights reserved. No reuse allowed without permission.

and a "groupable" characteristic (i.e., perceived as a whole)[28]. Crucially, our results suggest that these features are found not only in words, images of objects and strings of symbols but also in EEAG, supporting their potential representational value.

Remarkably, FUS4 was also the only region where the leftward asymmetry survived the FDR correction under the EEAG condition (mean = 0.12, t(25) = 3.17, p = 0.04 FDR corrected, one-sample two-sided t-test). As previously described[16], word presentation causes the largest leftward asymmetry likely due to hemisphere high-order language areas top-down processing leading to right FUS4 deactivation (Table 1). A significant, but lower intensity, leftward asymmetry was also present during the perception of objects and the linear B script (Figure 4A, all p's < 0.05 corrected, one-sample two-sided t-tests). The leftward asymmetries measured during the EEAG, linear B script and object presentations did not significantly differ (all p's > 0.10, post hoc t-tests) but were significantly larger than those measured during the scene perception (all p's < 0.01) and significantly smaller than those triggered in the words minus scrambled words contrast (all p's < 0.0001). To ensure that this result was not determined by variation under the scrambled pictures conditions, we confirmed that the perception of the scrambled pictures of each category did not result in any significant asymmetry in this region (compared to the fixation dot, see methods, all p's > 0.10 uncorrected, Figure 4B).

Importantly, the left hemisphere hosts language in most right-handed individuals. More generally, the left hemisphere is dedicated to cultural artifacts processing in most humans[30]. Under this framework, the leftward asymmetry observed in FUS4 during the perception of EEAG suggests that EEAG share some representational features with both objects and the linear B script that are not present in scenes, which did not show any asymmetry (p = 0.72, one-sample two-sided t-test). The trend of gradually decreasing leftward asymmetries in FUS4 from words, objects, linear B characters, EEAG to scenes may reflect the meaning conveyed by the different categories of stimuli; i.e., the more a stimulus is identified as conveying meaning, the more important the leftward asymmetry (Figure 4). This finding can be considered additional evidence supporting that EEAG are recognized as forms that could have been used by a human culture in the past to store and transmit coded information. Thus, the human brain perceives these graphic entities as having significant regularities to which semantic information can be connected. The present results support the assumption that this type of production was not exclusively associated with anatomically modern humans.

Materials and methods

Participants

The study was approved by the "Sud-ouest outremer III" local Ethics Committee (N° 2016/63). Twenty-six healthy right-handed adults (mean age ± SD: 21.7 ± 2.5 years, 15 women) with no neurological history were included after providing written informed consent to participate in the study. The participants had a mean educational level of 15 years of schooling after first grade. One participant was excluded from the analysis due to technical issues in the fMRI images.

Data acquisition

Stimuli

Our experimental protocol included five categories of stimuli, and each category was compared to its scrambled version (Figure 1).

The stimuli of interest, labelled EEAG, consisted of 50 tracings of abstract patterns created with stone tools on a variety of media that were discovered at archaeological sites dating from the Lower, Middle and Early Upper Palaeolithic eras (see Table S1 in supplementary material). We used tracings in which the engraved lines were rendered in white on a grey background and the outline of the object was rendered in light grey. The thickness of the lines on the tracings reflects the width of the engraved lines on the original piece. These stimuli were 700 * 480 pixels in size.

The pictures of objects (256 * 256 pixels) were represented by/consisted of nameable human-made artefacts depicted in different shades of grey. The stimuli were used to determine whether the neural bases of the engravings' perception can be distinguished according to their levels of perceptual organization and the meaning they convey. The lowest level of organization was represented by the scrambled pictures, which were designed to serve as a control for the processing of each condition. These stimuli were constructed by randomly scrambling the other pictures into 32 to 124 squares depending of the initial size of the original picture using MATLAB software (MathWorks, Inc., Sherborn, MA, USA). This treatment removes any perceptible organization from

bioRxiv preprint doi: https://doi.org/10.1101/464784; this version posted November 20, 2018. The copyright holder for this preprint (which was not certified by peer review) is the author/funder. All rights reserved. No reuse allowed without permission.

the images[19]. These stimuli were included as matched reference stimuli and used to subtract non-specific activations linked to the processing of any type of visual information (stimuli were equal in global luminance and size).

The corpus of linear B consisted of 50 images of six characters strings written in white on a grey background. These images were 653 * 114 pixels in size.

The word stimuli were bi-syllabic and composed of six letters in lowercase on a grey background. The word stimuli were nouns referring mostly to a concrete notion (80%). The pictures of words had a size of 256 * 64 pixels. The word frequency was 15.5 ± 3 (SD) according to the lexical data Lexicon 3[30]. Low frequency words were chosen since these words activate ventral occipito-temporal regions more strongly than frequent words[31].

The outdoor scenes were 256 * 256 pixels pictures of scenes, including the landscapes of mountains, beaches, or cities.

fMRI acquisition

The imaging was performed using a Siemens Prisma 3 Tesla MRI scanner. The structural images were acquired with a high-resolution 3D T1 weighted sequence (TR = 2000 ms, TE = 2.03 ms; flip angle = 8°; 192 slices; and 1 mm^3 isotropic voxel size). In addition B0 maps were acquired to correct for geometric distortion (two acquisitions of 18s repeated four times). The functional images were acquired with a whole-brain T2*-weighted echo planar image acquisition (T2*-EPI Multiband x6, sequence parameters: TR = 850 ms; TE = 35 ms; flip angle = 56°; 66 axial slices; and 2.4 mm^3 isotropic voxel size). The functional images were acquired in three sessions. The experiment presentation was programmed in E-prime software (Psychology Software Tools, Pittsburgh, PA, USA). The stimuli were displayed on a 27" screen. The participants viewed the stimuli through the rear of the magnet bore via a mirror mounted on the head coil.

Experimental protocol

The acquisition was organized in 3 sessions. The participants performed a 1-back task involving pictures of objects, scenes, and words and their scrambled versions in one session.

During the first run, the stimuli consisted of 234 distinct pictures presented in greyscale in a bitmap format belonging to one of the following three categories: scenes, objects, and words in their intact and scrambled versions. There were 39 different pictures per category. The block-designed paradigm consisted of 18 blocks lasting 12.75 s (6 blocks per category and their scramble version). Each of the 15 stimuli within a block was displayed for 300 ms, including two repetitions, and the participants were asked to detect the stimuli. A fixation point was displayed for 12.75 s every two blocks.

During the second and third runs, the subjects performed the same task, and the stimuli were the engravings, linear B strings and their scrambled version. Each run lasted for 4 min and 12 s with a random order of presentation and comprised 12 experimental blocks of 13.6 s interleaved with 7 fixation blocks of 12.75s. Each experimental block contained 11 stimuli and 2 repetitions with a 200 ms presentation time for each stimulus and an interstimulus interval of 1037 ms.

Image processing

Image analysis was performed using SPM12 software. The T1-weighted scans of the participants were normalized to a site-specific template (mean of 500 age-matched normal volunteers) matching the MNI space using the SPM12 "segment" procedure with the default parameters. To correct for subject motion during the fMRI runs, the 192 EPI-BOLD scans were realigned within each run using a rigid-body registration. Then, the EPI-BOLD scans were rigidly registered structurally to the T1-weighted scan. The combination of all registration matrices allowed for the warping of the EPI-BOLD functional scans to the standard space with a trilinear interpolation. Once in the standard space, a 6-mm FWHM Gaussian filter was applied.

Regional analysis

Within the selected hROIs, the activation profiles across the regions were calculated for each condition contrast (engravings minus scramble, objects minus scramble, scenes minus scramble, linear B minus scramble and words minus scramble) for each of the 26 participants.

The objects, linear B and scenes were compared to the engravings using repeated- measures 3-way ANOVA in each hemisphere (i.e., 2 (conditions) x 10 (hROIs)). In addition, Pearson's correlation coefficients between the profiles of the engravings and objects conditions were computed for each subject and Fisher z-transformed. Then, the 26

bioRxiv preprint doi: https://doi.org/10.1101/464784; this version posted November 20, 2018. The copyright holder for this preprint (which was not certified by peer review) is the author/funder. All rights reserved. No reuse allowed without permission.

Z-scores were analysed using a univariate two-sided t-test to determine whether the profile of objects was correlated to the profile of engravings. This analysis was conducted in each hemisphere separately.

A list of the regions activated by the objects, words, linear B, and scenes compared to their respective scrambled counterparts is presented in Table S3 to S6 as supplementary material.

Since a leftward asymmetry in the ventral route is typical of the processing of semantic and verbal material[16,27], we calculated the left minus right BOLD values in the selected hROIs during the EEAG presentations to identify the hROIs with significant leftward asymmetries (one-sample t-test, FDR corrected). Then, we compared the identified hROI(s) asymmetries across all conditions with one-way ANOVA.

Acknowledgements

This research was supported by a grant from IdEx Bordeaux / CNRS (PEPS 2015). The authors thank GinesisLab (Programme Labcom 2016, ANR 16LCV2-0006-01) for their help in data management and data processing and Carole Peyrin for providing some of the stimuli used.

Author contributions

EM, NTM and FE conceived the study. EM, MS, GJ, and AM designed the study. EM, MS, and SC performed the experiment, EM, MS, SC, NTM, MJ, and BM carried out the analyses, EM, NTM and FE wrote the manuscript with contributions from AM, BM, and GJ.

Competing interest

The authors declare no competing interests.

References

1. Klein, R. G. Archeology and the evolution of human behavior. Evolutionary Anthropology 9, 17-36 (2000).

2. Joordens, J. C. A. et al. Homo erectus at Trinil on Java used shells for tool production and engraving. Nature 518, 228-231 (2015).

3. Rodríguez-Vidal, J. et al. A rock engraving made by Neanderthals in Gibraltar. Proc Natl Acad Sci U S A 111, 13301-13306 (2014).

4. Hoffmann, D. L. et al. U-Th dating of carbonate crusts reveals Neandertal origin of Iberian cave art. Science 359, 912-915 (2018).

5. Henshilwood, C. S., d'Errico, F. & Watts, I. Engraved ochres from the middle stone age levels at Blombos Cave, South Africa. Journal of human evolution 57, 27-47 (2009).

6. Texier, P. J. et al. From the Cover: A Howiesons Poort tradition of engraving ostrich eggshell containers dated to 60,000 years ago at Diepkloof Rock Shelter, South Africa. Proc Natl Acad Sci U S A 107, 6180-6185 (2010).

7. Homo symbolicus: the dawn of language, imagination and spirituality (John Benjamins Publishing Company, 2011).

8. Aubert, M. et al. Pleistocene cave art from Sulawesi, Indonesia. Nature 514, 223-227 (2014).

9. Hodgson, D. Understanding the origins of Paleoart: the neurovisual resonance theory and brain functioning. Paleoanthropology 2006, 54-67 (2006).

10. Hodgson, D. Deciphering Patterns in the Archaeology of South Africa. Cognitive Models in Palaeolithic Archaeology 133 (2016).

11. Grill-Spector, K. & Weiner, K. S. The functional architecture of the ventral temporal cortex and its role in categorization. Nature Reviews Neuroscience (2014).

12. Downing, P. E., Chan, A. W.-Y., Peelen, M. V., Dodds, C. M. & Kanwisher, N. Domain specificity in visual cortex. Cereb Cortex 16, 1453-1461 (2006).

13. Köler, W. Gestalt Psychology New York (Liveright), 1929).

14. Koffka, K. Principles of Gestalt Psychology New York, 1935).

15. Jobard, G., Crivello, F. & Tzourio-Mazoyer, N. Evaluation of the dual route theory of reading: a metanalysis of 35 neuroimaging studies. Neuroimage. 20, 693-712 (2003).

bioRxiv preprint doi: https://doi.org/10.1101/464784; this version posted November 20, 2018. The copyright holder for this preprint (which was not certified by peer review) is the author/funder. All rights reserved. No reuse allowed without permission.

16. Vigneau, M., Jobard, G., Mazoyer, B. & Tzourio-Mazoyer, N. Word and non-word reading: What role for the Visual Word Form Area? Neuroimage. 27, 694-705 (2005).

17. Joliot, M. et al. AICHA: An atlas of intrinsic connectivity of homotopic areas. J Neurosci Methods 254, 46-59 (2015).

18. Haxby, J. V. et al. Distributed and overlapping representations of faces and objects in ventral temporal cortex. Science 293, 2425-2430 (2001).

19. Grill-Spector, K. The neural basis of object perception. Curr.Opin.Neurobiol. 13, 159- 166 (2003).

20. Grill-Spector, K., Kourtzi, Z. & Kanwisher, N. The lateral occipital complex and its role in object recognition. Vision research 41, 1409-1422 (2001).

21. Malach, R. et al. Object-related activity revealed by functional magnetic resonance imaging in human occipital cortex. Proc Natl Acad Sci U S A 92, 8135-8139 (1995).

22. Kim, J. G., Biederman, I., Lescroart, M. D. & Hayworth, K. J. Adaptation to objects in the lateral occipital complex (LOC): shape or semantics. Vision Res 49, 2297-2305 (2009).

23. Margalit, E., Biederman, I., Tjan, B. S. & Shah, M. P. What Is Actually Affected by the Scrambling of Objects When Localizing the Lateral Occipital Complex? J Cogn Neurosci 29, 1595-1604 (2017).

24. Ponce de León, M. S., Bienvenu, T., Akazawa, T. & Zollikofer, C. P. Brain development is similar in Neanderthals and modern humans. Curr Biol 26, R665-6 (2016).

25. Holloway, R. L. et al. Endocast morphology of Homo naledi from the Dinaledi Chamber, South Africa. Proc Natl Acad Sci U S A 115, 5738-5743 (2018).

26. Cohen, L. et al. The visual word form area: spatial and temporal characterization of an initial stage of reading in normal subjects and posterior split-brain patients. Brain 123, 291-307 (2000).

27. Price, C. J. & Devlin, J. T. The myth of the visual word form area. NeuroImage 19, 473- 481 (2003).

28. Vogel, A. C., Petersen, S. E. & Schlaggar, B. L. The left occipitotemporal cortex does not show preferential activity for words. Cereb Cortex 22, 2715-2732 (2012).

29. Vogel, A. C., Petersen, S. E. & Schlaggar, B. L. The VWFA: it's not just for words anymore. Front Hum Neurosci 8, 88 (2014).

30. New, B. Lexique 3 : Une nouvelle base de données lexicales. Verbum ex machina. Actes de la 20e conférence sur le Traitement Automatique des Langues Naturelles

31. Kronbichler, M. et al. The visual word form area and the frequency with which words are encountered: evidence from a parametric fMRI study. NeuroImage 21, 946-953 (2004).

bioRxiv preprint doi: https://doi.org/10.1101/464784; this version posted November 20, 2018. The copyright holder for this preprint (which was not certified by peer review) is the author/funder. All rights reserved. No reuse allowed without permission.

Supplementary materials

Site	Region	Material	No. of objects	Cultural Attribution	Age (kyr BP)	Description	Reference
Africa							
Blombos	South Africa	Ochre; Bone	18	MSA	100-75	CH; PAR; CC	d`Errico et al. 2001; Henshilwood et al. 2002, 2009
Diepkloof	South Africa	OES	7	MSA	65-55	SPL; CL; CHB	Texier et al. 2010
Klasies River	South Africa	Ochre	1	MSA II	100-85	SPL	d'Errico et al. 2012
Klein Kliphuis	South Africa	Ochre	1	MSA	80-50	SPL; CH	Mackay and Welz 2008
Klipdrift Shelter	South Africa	OES	1	MSA	65–59	CH; CC; SPL	Henshilwood et al. 2014
Pinnacle Point	South Africa	Ochre	1	MSA	100	SPL	Watts 2010
Palmenhorst	Namibia	Stone	1	MSA	Undated	CH; CC; PAR	Henshilwood and d'Errico 2011
Sibudu Cave	South Africa	Ochre	3	MSA	77-58	PAR; FL	Hodgskiss 2014
Europe							
Bacho Kiro	Bulgaria	Bone	1	MP-M	>47	ZZ	Marshack 1976, 1982
Bilzingsleben	Germany	Bone	2	LP	412-320	SPL; FL	Mania and Mania 1988
Ermitage	France	Bone	1	MP-M	>31	PAR; SPL	Pradel and Pradel 1954; d`Errico 1998
Gorham`s Cave	Gibraltar	Bedrock	1	MP-M	>39	CH	Rodríguez-Vidal et al. 2014
Kiik-Koba	Crimea	Flint	1	MP-PM	35-37	SPL	Stepanchuk 2006, Majkić et al. 2018
Kozarnika	Bulgaria	Bone	1	LP	900	PMK	Sirakov et al. 2010; Ivanova 2009; Guadelli and Guadelli 2004
Krapina	Croatia	Bone	1	MP	130	PMK	Frayer et al. 2006
La Ferrassie	France	Bone	1	MP-M	65	PMK	Capitan and Peyrony 1912; Zilhao 2007
Mamontovaya Kurya	Russia	Tusk	1	MP-M	36	SPL	Pavlov et al. 2001; Svendsen, Pavlov 2003
Pešturina	Serbia	Bone	1	MP-Ch/Qt	95–64	SPL	Majkić et al. 2017
Temnata Dupka	Bulgaria	Stone slab	1	MP	50	PAR	Cremades et al. 1995; Tsanova 2006
Middle East							
Qafzeh	Israel	Flint	1	MP-M	100	PAR	Hovers et al. 1997
Quneitra	Israel	Flint	1	MP-M	50	CO	Goren-Inbar 1990; Marshack 1996; d`Errico et al. 2003
Asia							
Shuidonggou	China	Stone	1	EUP	30	PAR	Peng et al. 2012
Trinil	Indonesia	Shell	1	LP	540-430	ZZ; PAR	Joordens et al. 2015

Table S1. Contextual and descriptive data on early engravings used as visual stimuli. CC: Criss-cross; CH: Cross-hatching; CHB: Cross hatched band; Ch/Qt: Charentian – Quina type; CL: Curved lines; CO: Concentric lines; EUP: Early Upper Paleolithic; FL: Fan-like; HB: Hatched band; LP: Lower Paleolithic; MP: Middle Paleolithic; M: Mousterian; MSA: Middle Stone Age; OES: Ostrich egg shell; PAR: Parallel lines; PM: para-Micoquian; PMK: Parallel marks; SPL: Sub-parallel lines; ZZ: Zigzag.

bioRxiv preprint doi: https://doi.org/10.1101/464784; this version posted November 20, 2018. The copyright holder for this preprint (which was not certified by peer review) is the author/funder. All rights reserved. No reuse allowed without permission.

hROI	Abreviation	Left hemisphere	Right hemisphere
		MNI coordinates	MNI coordinates
G_Fusiform-2	FUS2	-35 -26 -23	38 -25 -24
G_Fusiform-3	FUS3	-37 -32 -24	37 -31 -24
G_Fusiform-4	FUS4	-43 -50 -17	44 -46 -18
G_Temporal_Inf-4	T3-4	-50 -61 -8	54 -58 -11
G_Fusiform-5	FUS5	-31 -50 -12	32 -47 -11
G_Temporal_Inf-5	T3-5	-45 -64 6	49 -58 4
G_Occipital_Inf-1	O3-1	-48 -69 –4	50 -60 -9
G_Occipital_Inf-2	O3-2	-45 -71 -7	47 -65 -7
G_Occipital_Mid-2	O2-2	-37 -77 14	41 -73 12
G_Occipital_Lat-3	OLat3	-40 -84 -12	43 -81 -12

Table S2. Abbreviations and MNI Coordinates of the mass center of the ten hROIs of the Aicha atlas activated by the perception of engravings minus scramble contrast.

bioRxiv preprint doi: https://doi.org/10.1101/464784; this version posted November 20, 2018. The copyright holder for this preprint (which was not certified by peer review) is the author/funder. All rights reserved. No reuse allowed without permission.

Table S3. Mean BOLD value of the hROIs activated in the Words minus scrambled words contrast ($p < 0.05$ uncorrected)

Activation of words minus scrambled words								
	Left hemisphere				Right hemisphere			
	Mean BOLD	SD	t	p	Mean BOLD	SD	t	p
G_Fusiform-1	0.11	0.02	4.40	0.0002				
G_Fusiform-2	0.07	0.03	2.27	0.0323				
G_Fusiform-4	0.25	0.06	4.22	0.0003				
G_Temporal_Sup-4	0.19	0.04	4.42	0.0002				
G_Temporal_Mid-4	0.14	0.04	3.21	0.0036				
G_Temporal_Inf-3	0.18	0.05	3.50	0.0018				
S_Sup_Temporal-4	0.32	0.05	6.13	<.0001				
S_Sup_Temporal-3					0.19	0.05	3.48	0.0019

Table S4. Mean BOLD value of the hROIs activated in the scenes minus scrambled scenes contrast ($p < 0.05$ uncorrected)

Activation of scene minus scrambled scene								
	Left hemisphere				Right hemisphere			
	Mean BOLD	SD	t	p	Mean BOLD	SD	t	p
S_Orbital-2					0.12	0.03	3.82	0.0008
G_Occipital_Lat-3					0.14	0.06	2.15	0.0411
G_Occipital_Lat-5	0.12	0.04	3.05	0.0054	0.18	0.04	4.56	0.0001
G_Occipital_Mid-1	0.31	0.05	6.69	<.0001	0.28	0.05	5.69	<.0001
G_Occipital_Mid-2	0.21	0.04	5.71	<.0001	0.20	0.04	5.40	<.0001
G_Occipital_Mid-3	0.25	0.04	6.74	<.0001	0.24	0.04	6.78	<.0001
G_Occipital_Mid-4	0.50	0.06	9.05	<.0001	0.43	0.06	7.49	<.0001
G_Occipital_Inf-2	0.12	0.04	2.92	0.0072	0.15	0.05	3.27	0.0032
G_Lingual-1	0.51	0.05	10.28	<.0001	0.43	0.04	10.03	<.0001
G_Lingual-2	0.23	0.05	4.87	<.0001	0.24	0.04	5.77	<.0001
G_Fusiform-2	0.07	0.02	2.89	0.0079	0.12	0.02	5.40	<.0001
G_Fusiform-3	0.06	0.03	2.14	0.0421	0.10	0.03	3.91	0.0006
G_Fusiform-4	0.10	0.05	2.11	0.0455	0.11	0.04	3.04	0.0055
G_Fusiform-5	0.31	0.04	7.09	<.0001	0.44	0.05	9.48	<.0001
G_Fusiform-6	0.10	0.04	2.65	0.0139	0.21	0.04	4.78	<.0001
G_ParaHippocampal-1					0.21	0.05	3.87	0.0007
G_ParaHippocampal-2	0.30	0.04	8.03	<.0001	0.29	0.04	6.52	<.0001
G_ParaHippocampal-4	0.33	0.05	6.46	<.0001	0.33	0.05	5.99	<.0001
G_ParaHippocampal-5	0.56	0.05	10.66	<.0001	0.53	0.04	12.13	<.0001
G_Temporal_Mid-4					0.13	0.04	2.83	0.0090
G_Temporal_Inf-5					0.09	0.03	2.89	0.0078
N_Thalamus-9	0.12	0.05	2.34	0.0276	0.16	0.04	4.44	0.0002
S_Sup_Temporal-4								

bioRxiv preprint doi: https://doi.org/10.1101/464784; this version posted November 20, 2018. The copyright holder for this preprint (which was not certified by peer review) is the author/funder. All rights reserved. No reuse allowed without permission.

Table S5. Mean BOLD value of the hROIs activated in the linear B minus scrambled linear B contrast ($p < 0.05$ uncorrected)

Activation of linearB minus scrambled linearB								
	Left hemisphere				Right hemisphere			
	Mean BOLD	SD	t	p	Mean BOLD	SD	t	p
S_Orbital-1					0.10	0.04	2.62	0.0146
S_Sup_Frontal-5					0.15	0.05	2.71	0.0120
S_Inf_Frontal-1	0.17	0.08	2.08	0.0482				
G_Frontal_Sup-3	0.17	0.05	3.72	0.0010				
G_Frontal_Mid-5	0.21	0.07	2.91	0.0075	0.18	0.07	2.58	0.0163
G_Frontal_Mid-4					0.23	0.08	2.91	0.0076
G_Frontal_Mid_Orb-1					0.22	0.09	2.47	0.0209
G_Frontal_Mid_Orb-2	0.31	0.08	3.80	0.0008	0.22	0.08	2.79	0.0100
G_Frontal_Sup_Medial-3	0.18	0.05	3.32	0.0028	0.18	0.06	3.04	0.0055
G_Occipital_Inf-1	0.19	0.09	2.18	0.0388				
G_Occipital_Inf-2	0.33	0.07	4.94	<.0001	0.26	0.06	4.25	0.0003
G_Occipital_Lat-3	0.32	0.08	3.81	0.0008	0.42	0.10	4.21	0.0003
G_Occipital_Lat-5	0.12	0.06	2.24	0.0344				
G_Lingual-5	0.16	0.07	2.16	0.0408				
G_Fusiform-3	0.14	0.04	3.67	0.0012	0.11	0.03	4.24	0.0003
G_Fusiform-4	0.40	0.07	5.65	<.0001	0.23	0.04	5.28	<.0001
G_Fusiform-5	0.14	0.04	3.17	0.0040				
G_Fusiform-6	0.14	0.04	3.39	0.0023				
G_Fusiform-7	0.14	0.06	2.47	0.0207				
G_Temporal_Mid-2					0.17	0.05	3.55	0.0016
G_Temporal_Inf-3	0.21	0.07	3.13	0.0045				
G_Parietal_Inf-1	0.31	0.09	3.50	0.0018	0.32	0.09	3.56	0.0015
G_SupraMarginal-6	0.24	0.09	2.65	0.0138	0.20	0.09	2.24	0.0339
G_SupraMarginal-7					0.27	0.09	3.11	0.0046
G_Angular-1					0.38	0.09	4.10	0.0004
N_Caudate-5	0.19	0.07	2.61	0.0150	0.21	0.08	2.83	0.0090
N_Thalamus-2	0.14	0.07	2.11	0.0451				

bioRxiv preprint doi: https://doi.org/10.1101/464784; this version posted November 20, 2018. The copyright holder for this preprint (which was not certified by peer review) is the author/funder. All rights reserved. No reuse allowed without permission.

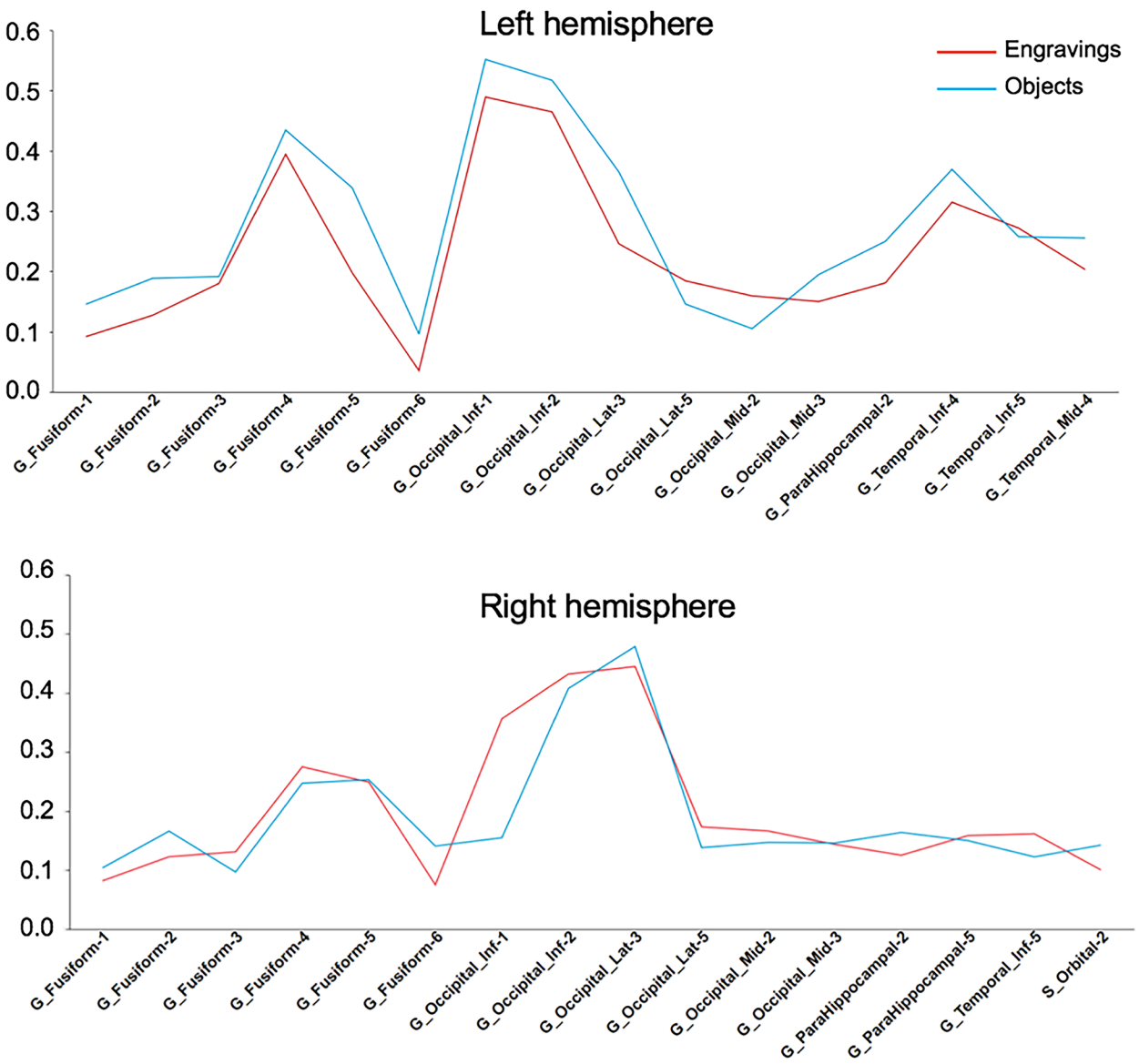

Figure S1. Descriptive analysis of the activation profiles under the Object and EEAG perception conditions of the 16 hROIs of the ventral route activated by object perception. No regions x conditions interaction was significant neither in the left nor in the right hemisphere ($F(15,375) = 1.25$, $p = 0.23$ and $F(15,375) = 1.15$, $p = 0.31$, respectively).